Old Sections 6.5 (b) and (c) PhL 10.7.14

Replaced by new text on 10.7.14.

(b) The Proximity Effect

Appendix D computes the E fields inside a round wire of radius a in terms of the surface charge moments η_m under the assumption that a wave $e^{j(\omega t-kz)}$ is traveling down the wire. We first remind the reader of the parameters involved. From (D.2.2),

$$\beta'^2 \equiv \beta^2 - k^2 \qquad \textit{(D.2.2)}$$

where

$$\beta = e^{j3\pi/4}(\sqrt{2}/\delta) = (j-1)/\delta = e^{j3\pi/4}\sqrt{\omega\mu\sigma} \qquad \textit{(2.2.30)}$$

$$k = -j\sqrt{\mathbf{zy}} = -j\sqrt{(R+j\omega L)(G+j\omega C)}\ . \qquad \textit{(5.3.5)} \qquad (6.5.8)$$

Here β is the wavenumber in the conductor medium shown in (1.5.1c), while k is a low-loss effective wavenumber for the transmission line wave having the form $e^{j(\omega t-kz)}$. Although k is a free parameter in Appendix D, it is forced equal to $-j\sqrt{\mathbf{zy}}$ in Chapter 5 where the Helmholtz equation is separated into longitudinal and transverse parts. This identification $k = -j\sqrt{\mathbf{zy}}$ is established only for high frequencies (= low-loss), but can be assumed approximately true at lower frequencies. This subject is discussed in detail in Section D.11 (a), and the high and low ω limits of k are obtained in Appendix Q. At high ω one sees that

$$k \approx -j\sqrt{(j\omega L)(j\omega C)} = -j\omega\sqrt{-LC} = +\omega\sqrt{LC} \approx \omega\sqrt{L_e C} = \omega/v_d \equiv \beta_{d0} \qquad \textit{(4.12.26)}$$

$$\beta'^2 \equiv \beta^2 - k^2 \approx -j\omega\mu\sigma - \beta_{d0}^2 \approx -j\omega\mu\sigma = \beta^2$$

where we identify $1/\sqrt{LC}$ with v_d, the speed of light in the dielectric, as shown in (4.12.19). The fact that $\beta^2 = -j\omega\mu\sigma$ is shown below (D.2.2) to be valid for $f << 10^{18}$ Hz, so for any reasonable large ω we do have

$$\beta' = \beta = e^{j3\pi/4}(\sqrt{2}/\delta) = (j-1)/\delta = e^{j3\pi/4}\sqrt{\omega\mu\sigma}\ . \qquad (6.5.9)$$

Now, since $n(\theta)$ is real and an even function of θ for our two-cylinder transmission line, $\eta_{-m} = \eta_m$ and from (D.10.4a) the longitudinal field $E_z(r,\theta)$ is shown to be

$$E_z(r,\theta) = (1/4)\, I\, R_{dc}\, (a\beta')\, [\, f_0(r) + 2\,\Sigma_{m=1}^{\infty}\, f_m(r)\, \eta_m\, \cos(m\theta)\,]\ . \qquad \textit{(D.10.4a)}$$

Using (6.5.4) for the η_m we then get

$$E_z(r,\theta) = I\, R_{dc}\, (\beta a/4)\, [\ f_0(r) + 2\,\Sigma_{m=1}^{\infty}\, (-1)^m\, e^{-m|\xi_1|}\, f_m(r)\, \cos(m\theta)\,] \qquad (6.5.10)$$

and then, since $R_{dc} = (1/\pi a^2\sigma)$,

$$J_z(r,\theta) = \sigma E_z(r,\theta) = (I/\pi a^2)(\beta a/4)\left[f_0(r) + 2\sum_{m=1}^{\infty} (-1)^m e^{-m|\xi_1|} f_m(r)\cos(m\theta)\right]$$

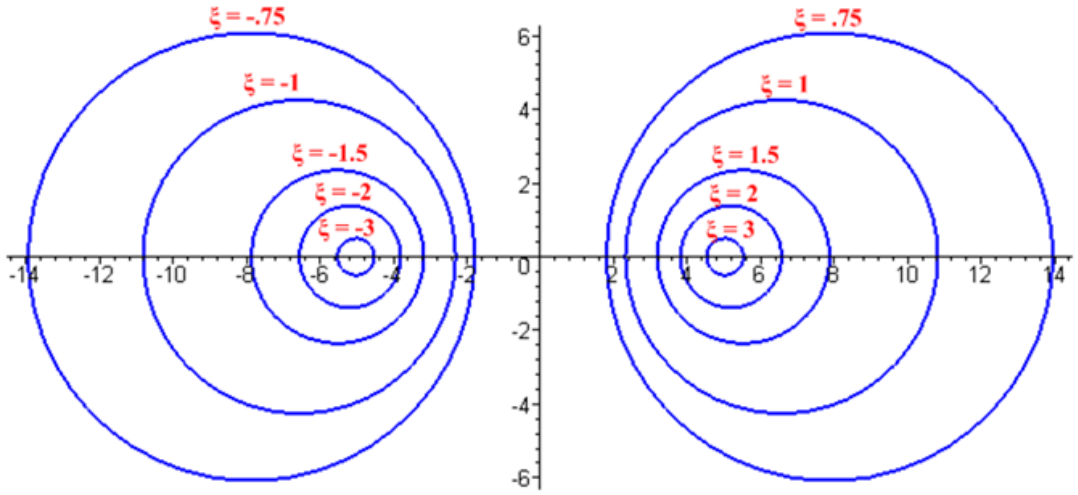
where

$$f_m(r) \equiv \left[\frac{J_m(x)}{J_{m+1}(x_a)} - \frac{J_m(x)}{J_{m-1}(x_a)}\right] \qquad x = \beta r \qquad x_a = \beta a \qquad \beta = e^{j3\pi/4}(\sqrt{2}/\delta) \ . \qquad (6.5.11)$$

This is the longitudinal current density in the left round conductor (the one with $\xi_1 < 0$) and just the fact that it is not constant in θ shows that we have a **proximity effect** as illustrated in Fig 6.6 above. We refer to this current density J_z as being "asymmetric" as opposed to "uniform".

(c) Plots of the Proximity and Skin Effects

First, it is helpful to have a plot showing the conductors for various values of ξ so one can get a feel for how "fat" the cylinders are relative to their separation distance (same as Fig 6.2),



Bipolar (2.5) Fig 6.10

From (6.5.11), using $J_{dc} = (I/\pi a^2)$,

$$J_z(r,\theta) = J_{dc}\ (\beta a/4)\left[f_0(r) + 2\sum_{m=1}^{\infty} (-1)^m e^{-m|\xi_1|} f_m(r)\cos(m\theta)\right] \ . \qquad (6.5.12)$$

In Maple code we first enter all the expressions of interest:

J_z = (6.5.12) β = (6.5.9) f_m = (6.5.11) η_m = (6.5.4) $x = \beta r$ $x_a = \beta a$

```
restart; alias(J=BesselJ,I=I,j=sqrt(-1));
```

```
Jz := Jdc * (beta*a/4)*( f(0) + 2*Sum(eta(m)*f(m)*cos(m*theta),m=1..N) );
```

$$Jz := \frac{1}{4} Jdc\ \beta\ a \left(f(0) + 2 \left(\sum_{m=1}^{N} \eta(m)\, f(m)\, \cos(m\,\theta) \right) \right)$$

```
beta := exp(j*3*Pi/4) * sqrt(2) / delta;
```

$$\beta := \frac{\left(-\frac{1}{2}\sqrt{2} + \frac{1}{2} j \sqrt{2} \right) \sqrt{2}}{\delta}$$

```
f:= m ->J(m,x)/J(m+1,xa) -  J(m,x)/J(m-1,xa);
```

$$f := m \rightarrow \frac{J(m, x)}{J(m+1, xa)} - \frac{J(m, x)}{J(m-1, xa)}$$

```
eta := m -> (-1)^m*exp(-m*abs(xi1));
```

$$\eta := m \rightarrow (-1)^m\, \mathbf{e}^{(-m\,|\xi 1|)}$$

```
x := beta*r:  xa := beta*a:
```

Next, specific parameters are entered (xi1 = ξ_1 = -1 and δ/a = 1/10),

```
N := 10:        # number of terms in sum
Jdc := 1:       # normalized DC current
xi1 := -1.00:   # label for left cylinder
a := 10:        # wire radius
delta := 1:     # skin depth
```

The first plot is of $|J_z(r,\theta)|$ where the axes are r and θ :

```
plot3d(abs(evalf((Jz))),r = 0..a,theta = 0..2*Pi, axes = boxed);
```

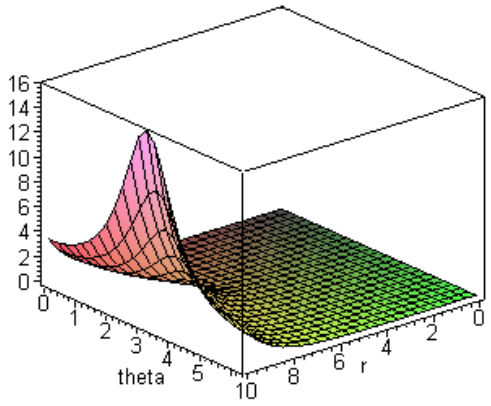
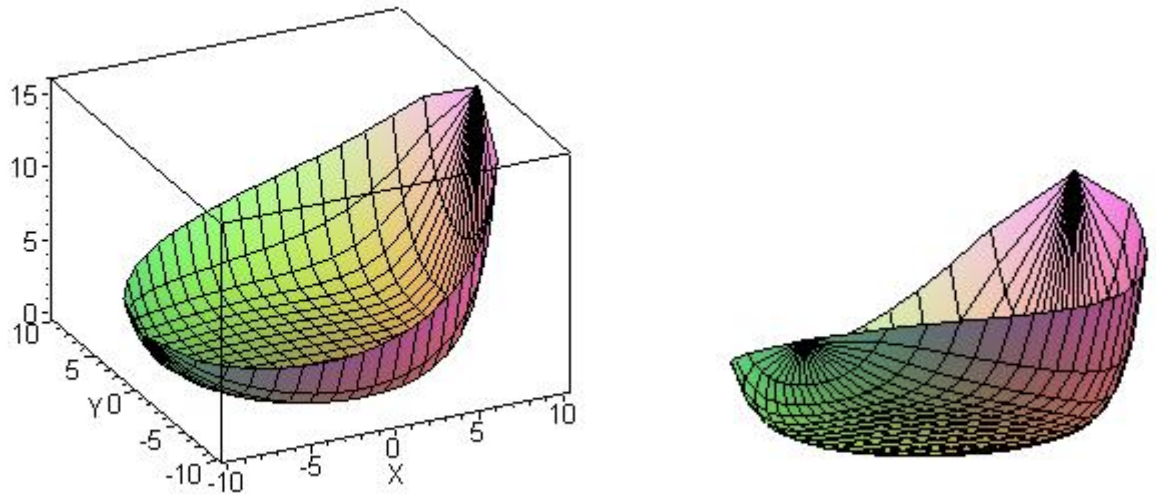


Fig 6.11

This shows the general peaking of $|J_z(r,\theta)|$ at θ = π (see Fig 6.7) , but the plot we really want to see is $|J_z(r,\theta)|$ displayed over the cross section of the round wire:

```
r := sqrt(X^2+Y^2):
theta := arctan(Y,-X):    # note that X = -r*cos(theta) for left wire
plot3d(abs(evalf(Jz)),X = -a..a,Y = -sqrt(a^2-X^2)..sqrt(a^2-X^2), axes = boxed,
grid = [20,20]);
```



$|J_z|$ Distribution in left round wire for a = 10, δ = 1 and ξ_1 = - 1.00 Fig 6.12

Observations:

• Skin effect for $|J_z|$ appropriate to δ/a = 1/10 is seen in the cross section. The "bottom" of the plot is flat at value 0 and indicates no current in the central conductor region -- all current is in the sheath of thickness ≈ 1 just inside the wire radius a = 10.

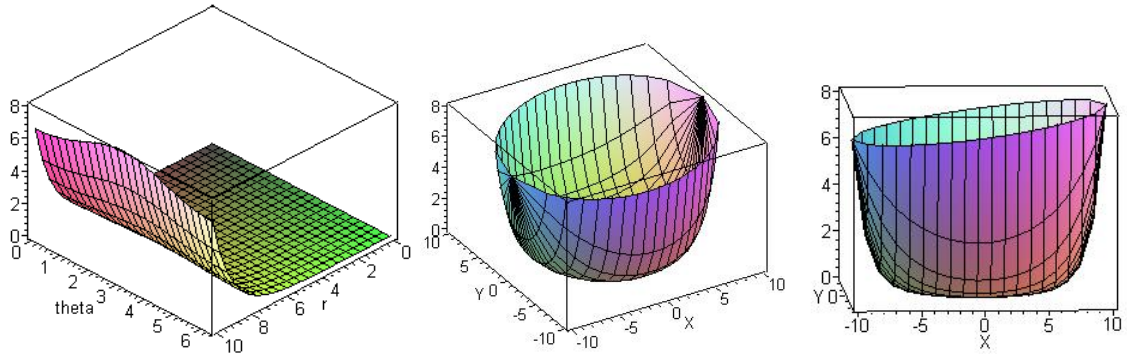
• The distribution is strongly peaked on the side of the conductor facing the other conductor; this is the proximity effect (currents in opposite directions).

• Using the formula given in (P.10.7),

$$\mathcal{R} = \mathcal{R}_{dc} \frac{E(J_z^2)}{[E(J_z)]^2}, \qquad (P.10.7)$$

one can compute the effect wire resistance $\mathcal{R} > \mathcal{R}_{dc}$ using (6.5.11) for J_z. The high and low ω limits of f_m and $J_z = \sigma E_z$ appearing in Appendix D.10 and D.11 simplify this task if those limits are of interest.

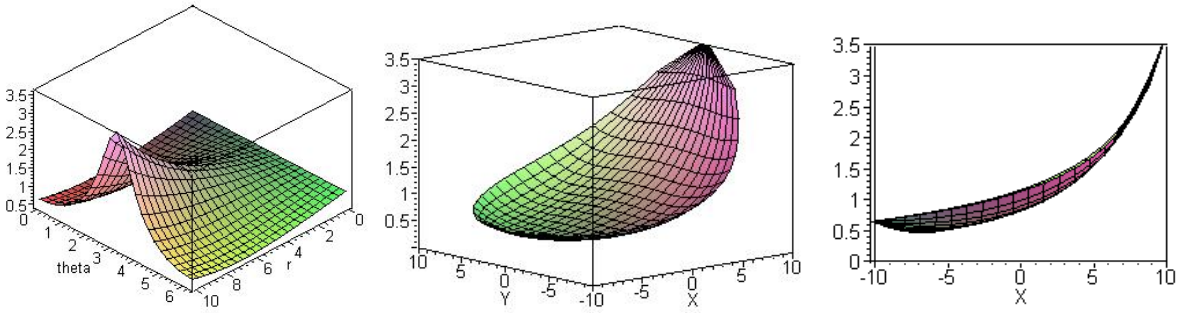
We now present a few such plots for different values of δ and ξ_1. First, for δ/a = 1/10 and ξ_1 = -3 :



$|J_z|$ Distribution in left round wire for a = 10, δ = 1 and ξ_1 = - 3.00 Fig 6.13

Here, for two equal-radius round wires of ξ_1= -3 and ξ_2= 3, the wires are "far apart" (see Fig 6.10 above). The proximity effect is still present as shown in the rightmost picture (larger at x = 10 than at x = -10), but the effect is small. On the other hand, the skin effect is still strongly in evidence, and again the entire current is in a sheath just inside r = a = 10 of thickness about δ = 1 unit.

Next is an example with δ/a = 1/2 and ξ_1 = -1 :



$|J_z|$ Distribution in left round wire for a = 10, δ = 5 and ξ_1 = - 1.00 Fig 6.14

In the central drawing we are looking into the bowl of the distribution from above. Since δ/a = 1/2 now, the skin effect is much less pronounced: J_z is no longer 0 in the central region as shown on the right. There is only a shallow "lip" around the bowl edge suggesting some skin effect. On the other hand, the proximity effect is still strong since for ξ_1 = -1 and ξ_2 = 1 the wires are fairly close together as shown in Fig 6.10. For such wires, using (6.5.6),

$$a/b = a_1/b = \frac{|\text{csch}\xi_1|}{\coth\xi_2 - \coth\xi_1} = \frac{|\text{csch}(-1)|}{\coth(1) - \coth(-1)} = \frac{\text{csch}(1)}{2\coth(1)} = \frac{1}{2\cosh(1)} = 0.324$$

$$\Longrightarrow \quad b/a = 3.08 \qquad \text{and} \qquad b/(2a) = 1.54$$

so the ratio of wire center separation to wire diameter is about 1.5 (which agrees with ruler measurements made on Fig 6.10 above). The two conductors touch when this ratio drops to 1.0.

In the next plot, we have a = 10 and δ = 1, but now we plot the value of $|J_z|$ at r = a going around the surface of the conductor for a set of different ξ_1 values:

```
r := a: N := 30:
plot([seq(abs(evalf(Jz)),xi1 = [-0.25,-0.5,-.75,-1,-1.5,-3])],theta =
0..2*Pi,color=red);
```

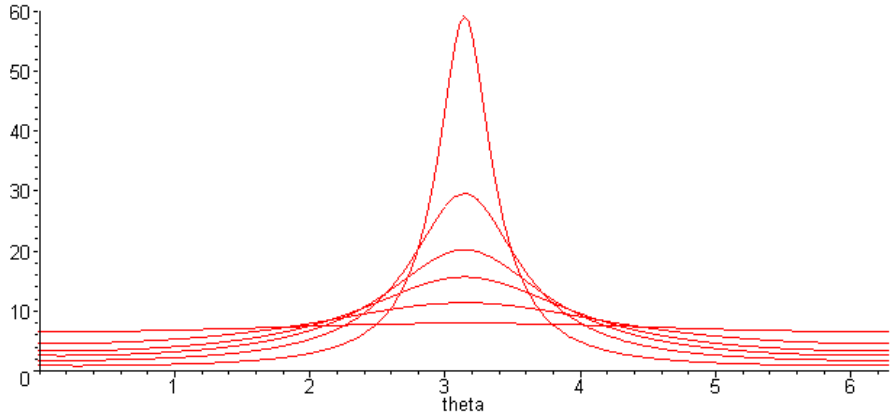


Fig 6.15

These plots of $|J_z|$ bear a strong resemblance to the surface charge density plots shown above in Fig 6.9 for the same set of ξ_1 values. It is shown in (D.10.15) that in the extreme skin effect regime we have

$$J_z(r,\theta) = -(j\omega)(\beta/\beta_{d0})\sqrt{\frac{a}{r}}\, e^{(1+j)(r-a)/\delta}\, n(\theta) \qquad \text{large } \omega \quad \textit{(D.10.15)} \qquad (6.5.13)$$

so we are not surprised to see that $J_z(r,\theta)$ tracks $n(\theta)$ in this manner. In the following section, we derive the above tracking relationship directly from div **E** = 0 .